Analysis of Polyolefins and Olefin Copolymers Using Crystaf Technique: Resolution of Crystaf Curves

Yury V. Kissin,[1] Hitesh A. Fruitwala[2]

[1]*Department of Chemistry, Rutgers-The State University of New Jersey, 610 Taylor Rd., Piscataway, New Jersy 08854*
[2]*ExxonMobil Chemical Company, Baytown Polymer Center, 5200 Bayway Drive, Baytown, Texas 77522*

Received 22 November 2006; accepted 21 May 2007
DOI 10.1002/app.27090
Published online 4 September 2007 in Wiley InterScience (www.interscience.wiley.com).

ABSTRACT: An experimental technique, crystallization analysis fractionation (Crystaf), is used to analyze compositional uniformity of ethylene/α-olefin copolymers and isotactic polypropylene. A computerized method for quantifying Crystaf data is developed based on resolution of Crystaf curves into their elemental components, with each component representing a fraction of the polymer with the same degree of chain imperfection. This analysis of Crystaf curves gives three parameters characterizing crystallizable polymer material: (a) the number of compositionally uniform components, (b) properties of each compositionally uniform component (in the case of ethylene/α-olefin copolymers, the comonomer content), and (c) the quantity of each component. Crystaf analysis of several ethylene/1-hexene copolymers produced with supported Ti-based Ziegler-Natta catalysts shows the existence of two groups of copolymer components. The first group includes components with low comonomer content, in the Crystaf analysis they precipitate at high temperatures as several relatively sharp peaks. The second group includes components with high comonomer contents; they precipitate at much lower temperatures, as a broad overlapping group of peaks. The peak resolution technique was applied to analysis of ethylene/α-olefin copolymers prepared with a supported catalyst at different temperatures, a copolymer produced with a pseudo-homogenous Ziegler-Natta catalyst, and to isotactic polypropylene. © 2007 Wiley Periodicals, Inc. J Appl Polym Sci 106: 3872–3883, 2007

Key words: crystallization fractionation; ethylene copolymers; polypropylene; Ziegler-Natta catalysts

INTRODUCTION

Monrabal developed the experimental technique named ''crystallization analysis fractionation'' (Crystaf) in the 1990s.[1,2] This technique is used for the analysis of compositionally homogeneous and inhomogeneous semicrystalline polymers such as polypropylene, poly(1-butene), ethylene/α-olefin copolymers with low α-olefin contents, etc.[1–4] In the Crystaf technique, a polymer is initially dissolved in an appropriate solvent at an increased temperature, then the temperature of solution is reduced very slowly resulting in gradual crystallization of the polymer. The concentration of the polymer remaining in solution is continuously monitored. The process is fully automated, and commercial equipment for Crystaf analysis is currently available. Crystaf analysis depends on the fact that the solution crystallization temperature of any semicrystalline polymer is primarily a function of two parameters. The first one is the chemical nature of a polymer: isotactic or syndiotactic polypropylene or poly(1-butene), olefin copolymers, etc. This parameter determines the overall crystallization range. The second parameter is the degree of structural uniformity of polymer chains: variation in the isotacticity degree of polypropylene, variation in the α-olefin content in ethylene/α-olefin copolymers, etc. In general, as the temperature of the solution is slowly decreased, polymer fractions begin to crystallize, first the more regular fractions and then the fractions with a lower degree of structural regularity. Positions of Crystaf peaks are also affected by molecular weights of the polymers (when the molecular weights are low, see the data for ethylene homopolymers below), but this effect is smaller than the two principal parameters.

Figure 1 shows a typical Crystaf trace for a compositionally nonuniform ethylene/1-hexene copolymer prepared with a supported Ti-based Ziegler-Natta catalyst (see details later). The average content of 1-hexene in the copolymer is 4.1 mol % (IR); its M_w is $\sim$ 70,000 and the M_w/M_n ratio is $\sim$ 5.3; its melt flow characteristics are: $I_2 = 4.0$, $I_{21}/I_2 = 32.1$. The figure gives the rate of polymer precipitation, dW/dT, as a function of solution temperature T. Typically, the ordinate value of such a curve starts at zero at the highest temperature, reaches a maximum, and then returns to some low value. In this particular case, the Crystaf curve consists of several closely positioned peaks. In this article, we provide a simple quantitative technique for the analysis of such multi-

Correspondence to: Y. V. Kissin (ykissin@rci.rutgers.edu) or H. A. Fruitwala (hitesh.a.fruitwala@exxonmobil.com).

Journal of Applied Polymer Science, Vol. 106, 3872–3883 (2007)

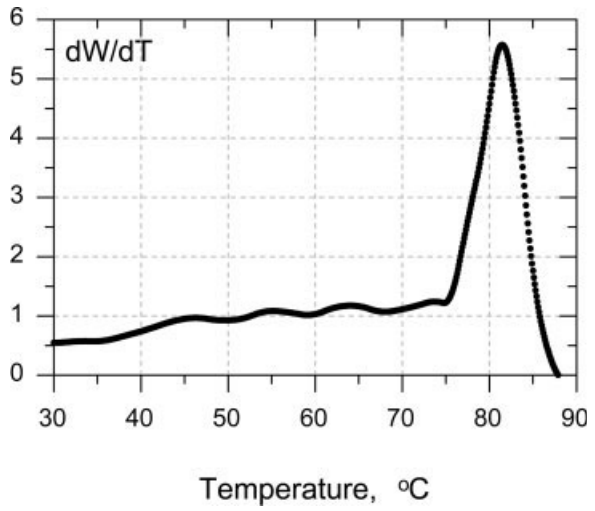

Figure 1 Crystaf curve of an ethylene/1-hexene copolymer prepared with a supported Ti-based Ziegler-Natta catalyst. C_{Hex} = 4.1 mol %.

component Crystaf curves. This technique is based on resolution of the curves into their elemental components, each component representing a fraction of a polymer with a similar degree of chain imperfection, either the same copolymer composition or the same degree of stereoregularity.

Ideally, the Crystaf analysis should provide four parameters:

1. The fraction of a polymer that remains dissolved at the lowest temperature of analysis. In the case of ethylene/α-olefin copolymers and polypropylene, these are completely amorphous materials.
2. The number of compositionally uniform Crystaf components.
3. Properties of each compositionally uniform component. In the case of ethylene/α-olefin copolymers, it is a copolymer composition; in the case of polypropylene and other polyolefins, it is stereoregularity of the component.
4. The relative content of each compositionally uniform component.

There was a previous attempt at resolving Crystaf curves of olefin copolymers into their constituent components.[2] It was based on the application of the Stockmayer bivariate distribution function.[5] This function theoretically describes a variation in the copolymer composition of different macromolecules (all produced by the same active center) as a function of their molecular weight. This theory predicts the Gaussian distribution of the deviation of copolymer compositions from the average composition and stipulates that the width of the distribution increases with the value of the reactivity ration product r_1r_2. The r_1r_2 values for ethylene/α-olefin copolymerization reactions with single-site metallocene catalysts are usually in a range from 0.2 to 0.5,[6] which predicts quite narrow Stockmayer compositional distributions for copolymers with M_w values over 50,000. To reconcile this prediction with quite broad Crystaf curves observed in experiments, the authors of Ref. 2 introduced empirical instrumental spreading corrections for Crystaf peaks.

Here, we present a simpler, empirical approach to modeling Crystaf peaks, which makes resolution of complex Crystaf curves, as that in Figure 1, amenable to curve-fitting programs run on personal computers.

EXPERIMENTAL PART

A number of ethylene/1-hexene and ethylene/1-octene copolymers were studied. Some of them were prepared in the laboratory, other were commercial LLDPE resins. Two groups of ethylene/1-hexene copolymers were analyzed: compositionally uniform copolymers prepared with the *n*-$BuCp_2ZrCl_2$–MAO system at high [Al] : [Zr] ratios, 2000 to 5000[7] and compositionally nonuniform copolymers prepared with several types of supported $TiCl_4$- and $TiCl_3$-based Ziegler-Natta catalysts.[8] Most materials of the latter type were synthesized in laboratory with a Ti-based silica-supported catalyst with a Ti content of 3 wt %.[9] The catalyst was prepared by treating silica with $MgBu_2$ at a 1.0 mmol/g ratio, followed by addition of $Si(OC_2H_5)_4$ at different [Si] : [Mg] ratios, from 0.4 to 0.85 (the reaction converts most Mg-Bu bonds into Mg-OC_2H_5 bonds) and, finally, with $TiCl_4$ at [Ti] : [Mg] = 1.0. Detailed procedures for performing the copolymerization reactions were described earlier.[10,11] Polypropylene samples were prepared under atmospheric pressure using a supported catalyst of the fifth generation, $TiCl_4/MgCl_2$/2,2-di-*i*-Bu-1,3-dimethoxypropane,[12] activated with $AlEt_3$.

Crystaf fractionation was carried out with a Model 110 Crystaf (Polymer Char) instrument. In the case of ethylene/α-olefin copolymers, 0.05 g of material was dissolved in 15 mL of 1,2,4-trichlorobenzene at 150°C; the solution was rapidly cooled to 100°C and then slowly cooled at a rate of 0.2°C/min to the final temperature, 30°C. The same procedure was used for polypropylene samples. The concentration of polymers remaining in solution was determined with an IR detector at 150°C. Parameters of the standard procedure are given in Table I. The initial polymer concentration is assigned the 100% value and a pure solvent (1,2,4-trichlorobenzene) is defined as 0%. Once the polymer solution has been cooled, the solution concentration is measured to determine the fraction that remains soluble at 30°C. This soluble frac-

TABLE I
Experimental Parameters of Crystaf Analysis for Ethylene/α-Olefin Copolymers

Process	Dissolution	Stabilization	Analysis	Sampling	Cleaning
Rate (°C/min)	25	25	0.20	0.20	30
Temp (°C)	160	100	70	30	170
Time (min)	60	45	0	0	15

tion is either an amorphous copolymer fraction with the α-olefin content >7–8 mol % or atactic polypropylene.

To obtain quantitative information on ethylene/α-olefin copolymers from the Crystaf data, a calibration curve was produced which relates the crystallization temperature of a copolymer fraction to the α-olefin content in the fraction. The calibration was performed by carrying out Crystaf analysis of two groups of ethylene/1-hexene copolymers. The first group included copolymers produced with single-center metallocene catalysts. The second group included two sets of very narrow fractions of compositionally nonuniform ethylene/1-hexene copolymers produced by the preparative Tref technique (temperature-rising elution fractionation[13–15]). Temperature ranges of the fractions and their compositions are listed in Table II. Copolymer compositions of the fractions were determined by ^{13}C NMR using a JEOL GX400 NMR spectrometer and by IR.[16] Several binary mixtures of the fractions were also analyzed by the Crystaf method. GPC analysis of the polymers was performed at 145°C with a Waters 150C Liquid Chromatograph (two columns 10^6, one each of 10^4 and 10^3 Å) using 1,2,4-trichlorobenzene as a solvent. Peak resolution in Crystaf curves and GPC curves was carried out with the Scientist program (MicroMath Scientific Software).

EXPERIMENTAL DATA AND DISCUSSION

Resolution of multicomponent Crystaf curves into peaks of compositionally uniform components

As Figure 1 shows, the Crystaf curve of a compositionally nonuniform ethylene/α-olefin copolymer consists of several strongly overlapping peaks. The peak resolution procedure we developed is based on a premise that such copolymers (as well as polypropylene samples produced with Ziegler-Natta catalysts, as described later) consist of several structurally distinct components. In the first approximation, we assumed that each such Crystaf component is compositionally uniform: all macromolecules in it have approximately the same copolymer composition or approximately the same stereoregularity. The goal of the resolution procedure is to determine structural properties of each Crystaf component and its relative content.

We approached the task of resolving multicomponent Crystaf curves using an experiment-based empirical method. Two sets of data for compositionally uniform polymers were used, the data for narrow fractions of ethylene/1-hexene copolymers produced by the preparative Tref method (see Table II) and the data for ethylene/α-olefin copolymers produced with single-center metallocene catalysts, both our own measurements of ethylene/1-hexene copolymers and the data for ethylene/1-octene copolymers given in Ref. 2.

Peak shape

The shape of an individual Crystaf peak (the rate of polymer precipitation, dW/dT, as a function of temperature T) can be reasonably well represented by the Gaussian distribution function with respect to T (see examples later):

$$dW_{peak}/dT = [(1/(\sigma_{Gauss}\sqrt{2\pi})] \times \exp[-(T_{max} - T)^2/2\sigma^2_{Gauss}] \quad (1)$$

where T_{max} is the temperature at a peak maximum for a given compositionally uniform component and σ_{Gauss} is the width parameter of the peak. In practice, most experimentally observed peaks of compositionally uniform materials are skewed toward low T values. A number of complex asymmetric broadening functions for Gaussian functions have been proposed in the literature.[17] We used a simple empirical approach: the skew was modeled as the sec-

TABLE II
Temperature Ranges of Fractions of Ethylene/1-Hexene Copolymer Prepared by Preparative Tref Method and their Compositions

Fraction	1	2	3	4	5	6	7	8	9
Temperature range (°C)	55–60	60–65	65–70	75–80	80–85	85–90	90–95	95–100	100–105
C_{Hex} (mol %)	5.4	4.9	4.8	2.5	1.9	1.3	0.5	~ 0.2	~ 0.1

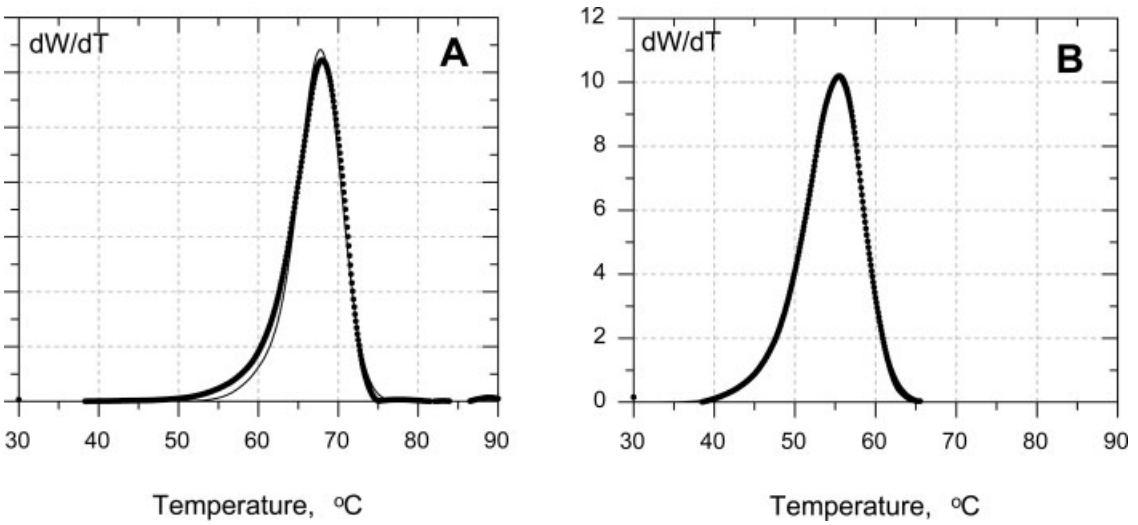

Figure 2 Crystaf curves of Tref fractions (points) and their modeling as single skewed Gauss curves. (A) 75–80°C fraction, (B) 65–70°C fraction.

ond Gaussian peak which is much smaller and broader. Its width parameter is σ_{skew} and the position of its maximum, $T_{max,2}$, is shifted to a lower temperature with respect to T_{max} by a δT value:

$$dW_{skew}/dT = R_{skew}[1/(\sigma_{skew}\sqrt{2\pi})] \times \exp\{-[(T_{max} - \delta T) - T]^2/2\sigma_{skew}^2\} \quad (2)$$

R_{skew} in eq. (2) is the ratio between the areas under the skew peak and the main Gaussian peak, A_{skew}/A_{Gauss}. The widths of the Gaussian peaks and the degree of their skewing depend on the position of the peak maximums, T_{max}: the lower is T_{max}, the broader and more skewed are the peaks. The same observation was made earlier in Ref. 2. These trends do not have any theoretical interpretation; therefore, we used our experimental data to develop empirical dependencies to represent the relationships for σ_{Gauss}, σ_{skew}, δT, and R_{skew} values as functions of T_{max}. They are described in Appendix. The Scientist program, by fitting experimental Crystaf peaks of compositionally uniform polymers with a sum of eqs. (1) and (2), gives the estimation of two parameters, the position of the main peak, T_{max}, and the total peak area, $A_{total} = A_{Gauss} \cdot (1 + R_{skew})$. Figure 2 shows two examples of the peak shape fitting.

Additional peak broadening for closely spaced peaks

An additional complication in resolving Crystaf peaks is caused by mutual cocrystallization effects when several compositionally uniform materials are present in a mixture. These effects were described recently by Soares and coworkers[18]: copolymer chains of similar compositions tend to co-crystallize and this results in broadening of Crystaf peaks of copolymer mixtures or even merging of the peaks when the peak positions of individual components are sufficiently close. This effect requires the introduction of an additional step in the modeling of Crystaf curves: accounting for peak broadening due to their proximity. This correction is especially important for ethylene/α-olefin copolymers produced with Ti-based Ziegler-Natta catalysts because these copolymers always contain components with different copolymer compositions, and the peaks of individual components are relatively close, as shown in Figure 1. Precipitation of a less soluble component in a mixture (which starts at a higher temperature) induces a more rapid precipitation of another, more soluble component; the latter begins precipitating at a somewhat higher temperature than that expected if only this second component alone is present in solution.

The magnitude of this effect was determined by analyzing several binary mixtures of compositionally uniform fractions. Figure 3(A) gives an example of this effect. Although the two fractions in the mixture have significantly different T_{max} values, $\Delta T_{max} = 16.5$°C, the interaction between the crystallization processes of the fractions is still observable: the peaks move closer together in mixtures (in this particular example, the gap between them decreases to ~ 14°C) and the second peak becomes much broader compared to the peak of the individual fraction. When two Crystaf peaks are positioned closer, the two peaks move even closer and both become noticeably broader, see Table III.

These examples show that when a Crystaf curve containing several relatively closely spaced peaks is analyzed, its modeling should take into account the effect of mutual peak broadening because of their

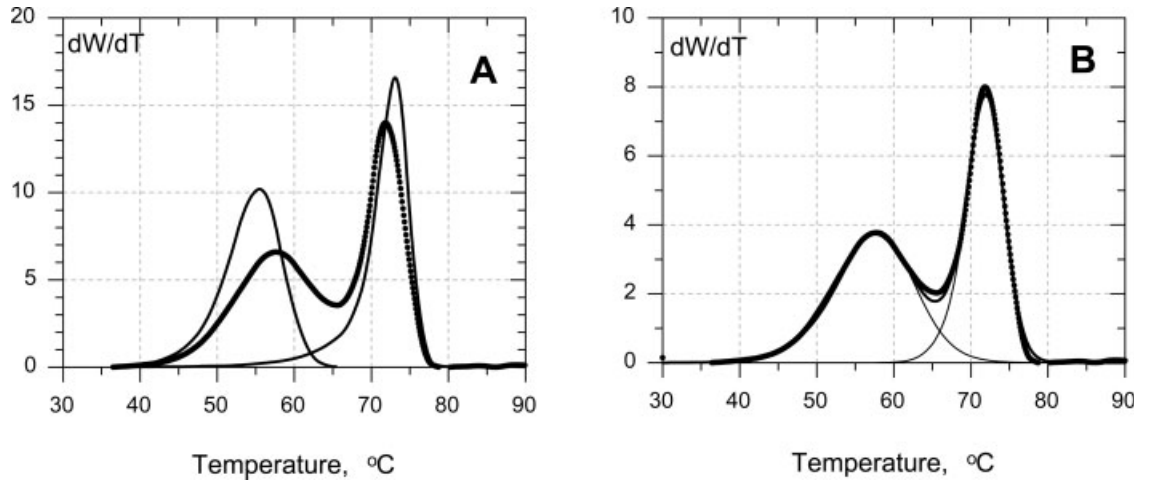

Figure 3 Mutual peak broadening of neighboring Crystaf peaks. (A) Crystaf peak of a 1 : 1 binary mixture of the 80–85°C and 65−70°C Tref fractions (points) and the peaks of its individual components (lines). (B) Modeling of the peak of the binary mixture with the program that takes into account peak proximity.

proximity. To this goal, we introduced several empirical peak-broadening corrections. Two parameters have to be corrected: (a) the widths of each Gaussian peak in a binary combination (this correction automatically results in broadening of the peaks' skew components), and (b) the fraction of the skew component for the peak with a higher T_{max}. This latter skew peak is positioned between the two overlapping main Gaussian peaks and an increase of its fraction fills the gap between the two closely spaced peaks, as shown in Figure 3(A). This additional peak broadening also depends on the relative areas of the peaks. The empirical correction functions are given in Appendix. An example of these corrections is shown in Figure 3(B).

Calibration of Crystaf method

The goal of calibration of Crystaf data is finding a relationship between the position of a peak on a Crystaf curve, T_{max}, and a structural property of the polymer material. We produced one such calibration dependence for ethylene/1-hexene copolymers. It relates the T_{max} value and the molar content of 1-hexene in the Crystaf component, C_{Hex} (mol %). The dependence is based on Crystaf analysis of a number of ethylene/1-hexene copolymers prepared with a single-center metallocene catalyst. Their compositions were measured by ^{13}C NMR and IR.[16] The calibration is shown in Figure 4. The plot can be approximated with reasonable accuracy by a linear dependence:

$$C_{Hex}(\text{mol}\,\%) = 10.073 - 0.1176 \cdot T_{max} \qquad (3)$$

In industry, another measure of copolymer composition is often used, the branching degree of polyethylene,[19] the number of methyl groups in a resin per 1000 carbon atoms, $CH_3/1000C$. The calibration dependence for it is:

$$CH_3/1000C = 45.378 - 0.5252 \cdot T_{max} \qquad (4)$$

TABLE III
Effects of Proximity of Crystaf Peaks on their Properties

	$T_{max,1}$ (°C)	Fraction 1 (%)	$T_{max,2}$ (°C)	Fraction 2 (%)
A. Mixture of fractions 3 (65–70°C) and 5 (80–85°C)				
Individual components	56.5	50.0	73.1	50.0
Data for mixture	58.3	49.5	72.2	50.5
B. Mixture of fractions 3 (65–70°C) and 4 (75–80°C)				
Individual components	56.5	50.0	68.0	50.0
Data for mixture	59.6	55.0	67.6	45.0

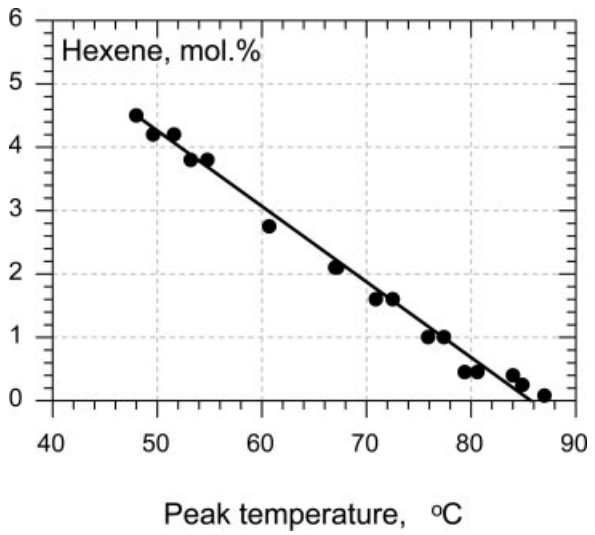

Figure 4 Crystaf calibration plot.

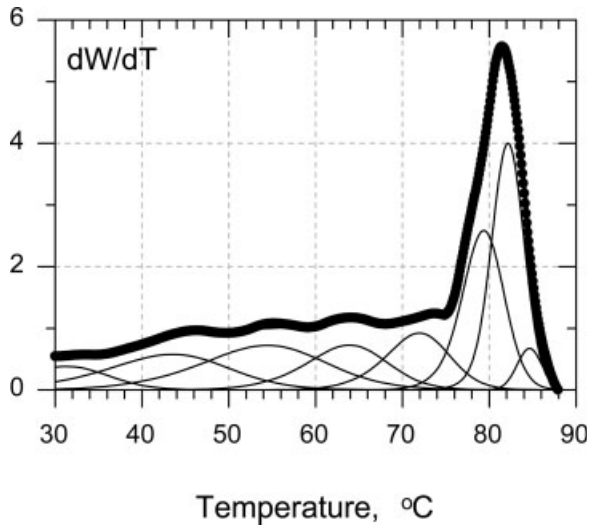

Figure 5 Resolution of Crystaf curve of ethylene/1-hexene copolymer produced with a supported Ziegler-Natta catalyst.

All these empirical correlations and the corrections for peak broadening for closely spaced peaks were introduced into a computer model of Crystaf curve resolution. A variety of copolymers can be analyzed using this approach. They include copolymers produced with various metallocene-based catalysts (as a tool for proving the single-center nature of these catalyst systems), copolymers prepared with various heterogeneous Ti-based catalysts, and copolymers prepared with pseudo-homogeneous Ziegler-Natta catalysts. The program is written for the Scientist data-fitting program. The outcome of the fitting is a list of Crystaf peak positions (T_{max} values) and relative contributions of the respective compositionally uniform components.

Examples of using the Crystaf resolution procedure

Figure 5 shows an example of modeling of a Crystaf curve of a compositionally nonuniform ethylene/1-hexene copolymer produced with a supported Ti-based catalyst (the same experimental curve as in Fig. 1). This example represents one of the most complex cases: eight elemental Crystaf curves are required to represent the data in an adequate manner. In addition, ~ 20% of the material, a completely amorphous copolymer fraction, remains dissolved in 1,2,4-trichlorobenzene at 30°C and cannot be fractionated using the Crystaf procedure. The parameters of the Crystaf components are listed in Table IV. The components are marked A to H in the order of decreasing T_{max} values. The compositions of the components, estimated with the calibration curve in Figure 4, show that this particular copolymer, which, on average, contains 4.1 mol % of 1-hexene, is in reality a mixture of copolymer molecules with widely different compositions, from materials with a very low 1-hexene content, 0.2–0.5 mol % (components A and B) to the fractions with a very high 1-hexene content, 5–6 mol % (components G and H).

Comparison of Crystaf and Tref data

Similar conclusions about the compositional range of individual fractions were reached earlier by using the analytical Tref method for analysis ethylene/1-butene copolymers prepared with a Ti-based catalyst,[20] and by analyzing combinations of GPC and kinetic data for ethylene/1-hexene copolymers.[10,16,21–23] Table V compares the results of Crystaf analysis of an ethylene/1-hexene copolymer produced with a $TiCl_4$-based silica-supported catalyst[9] (the average 1-hexene content on the copolymer is 1.9 mol %) and the results of Tref analysis of an ethylene/1-butene copolymer (from Ref. 19) produced with a similar $TiCl_4$-based silica-supported catalyst (the average 1-butene content on the copolymer is 3.5 mol %). On a qualitative level, similarities between the Crystaf and the analytical Tref method were noticed earlier.[4] The data in Table V show that resolution of both the Crystaf and the analytical Tref curves into elemental components can serve as the basis of a much more detailed, quantitative comparison of the two complimentary techniques. Both the analytical techniques identify copolymer components of similar compositions covering a broad range of α-olefin contents in the copolymers, from 0.3–0.5 mol % (Crystaf fractions A and B, Tref fractions 1 and 2, respectively) to ~ 6–8% (Crystaf fraction G, Tref fraction 6). Some differences exist in the compositions of the respective fractions, which can be explained by differences in the type of an α-olefin used in the copolymerization reactions (1-butene is nearly three times more reactive than 1-hexene in

TABLE IV
Crystaf Components of Ethylene/1-Hexene Copolymer Produced with Supported Ti-Based Ziegler-Natta Catalyst

Component	T_{max} (°C)	C_{Hex} (mol %)	Fraction (%)
A	84.0	~ 0.2	6.9
B	81.6	0.5	17.4
C	78.8	0.8	9.9
D	72.2	1.6	11.6
E	63.5	2.6	9.5
F	54.5	3.7	10.3
G	~ 44	4.8	9.2
H	~ 33	6.2	4.8
Soluble fraction[a]	–		20.4

[a] Does not precipitate from solution in 1,2,4-trichlorobenzene at 30°C.

TABLE V
Compositional Distribution Measurements in Ethylene/α-Olefin Copolymers Produced with Supported Ti-Based Ziegler-Natta Catalysts

A: Crystaf components of ethylene/1-hexene copolymer			
Component	T_{max} (°C)	C_{Hex} (mol %)	Fraction (%)
Conditions: 85°C, [hexene] : $[ethylene]_{mon}$ = 4.4 (molar), C_{Hex}(av.) = 1.9 mol %			
A	81.2	0.5	19.6
B	78.6	0.8	47.1
C	75.7	1.2	11.5
D	69.5	1.9	6.6
E	60.4	3.0	4.7
F	~ 49	4.3	4.2
G	~ 37	5.7	1.8
Soluble fraction[a]			4.4

B: Analytical Tref components of ethylene/1-butene copolymer[19,b]			
Component	T_{max} (°C)	C_{But} (mol %)	Fraction (%)
Conditions: 80°C, [butene] : $[ethylene]_{mon}$ = 1.6 (molar), C_{But}(av.) = 3.5 mol %			
1	93.1	0.3	15.5
2	90.5	0.8	37.0
3	86.8	1.5	16.9
4	78.0	3.1	20.3
5	70.0	4.6	6.0
6	50.0	8.6	4.4

[a] The fraction that does not precipitate at 30°C.
[b] ~ 10% of copolymer remains soluble at the lowest crystallization temperature, 50°C.

copolymerization with ethylene)[24] and by differences in catalyst recipes (the catalyst in the second example produces a significantly higher fraction of copolymer molecules with the α-olefin content in the range of 2–3 mol %).

Ethylene homopolymers

An ethylene homopolymer prepared with a supported $TiCl_4$-based catalyst containing 3 wt % of Ti[9] (see Experimental) was analyzed with the Crystaf method. The copolymer was prepared in a polymerization reaction under a high hydrogen concentration in order to reduce its molecular weight and to increase its solubility in halogenated aromatics. The Crystaf curve of the polymer was resolved into components as if it were the Crystaf curve of an ethylene/α-olefin copolymer. The result shows that ~ 85% of the material is represented by a single Crystaf peak and that its T_{max} value, 82.5°C, corresponds to a material with an ''α-olefin content'' of <0.1 mol %, i.e., a homopolymer. However, there are three other small components on the Crystaf curve of the homopolymer that represent crystallization of polyethylene fractions with very low molecular weights. This example underlines limitations of the Crystaf method in analyzing materials with very low molecular weights.

Temperature effect on ethylene/α-olefin copolymerization with a supported catalyst

Our earlier analysis of GPC data for ethylene/α-olefin copolymers[10,19–23] showed that all supported Ti-based catalysts contain several types of active centers which differ in the molecular weights of the material they produce under a given set of polymerization conditions and in the copolymer compositions of the respective fractions. For example, the copolymer compositions can vary from 0.3–0.4 mol % of an α-olefin for high molecular weight fractions to over 12–15 mol % for low molecular weight fractions. The later are completely amorphous and cannot be analyzed by the Crystaf method. This complex structure of ethylene/α-olefin copolymer fractions produced with Ti-based catalysts should result in complex, multicomponent Crystaf curves, the conclusion borne out by the experimental data (see Fig. V).

Table VI gives experimental conditions of two ethylene/1-hexene copolymerization reactions that were carried out with the same supported catalyst[9] at two different temperatures. These reaction conditions were chosen to prepare both copolymers at similar molar C_{Hex}/C_E ratios in the monomer mixture and at similar ethylene and hydrogen concentrations. Average properties of the copolymers, shown in Table VI, exhibit similar temperature effects as those reported earlier for copolymerization reactions with the same catalyst in the absence of hydrogen[25]: as the temperature of the reaction increases, the average molecular weight decreases (although the molecular weights of both copolymers are quite low in the presence of a large amount of hydrogen), and the 1-hexene content in the copolymer increases.

TABLE VI
Copolymerization of Ethylene and 1-Hexene with a Supported Ti-Based Ziegler-Natta Catalyst

Temp. (°C)	P_E (MPa)	C_{Hex}^{mon} (M)	$(C_{Hex}/C_E)_{mon}$	C_{Hex} (mol %)	M_w	M_w/M_n
75	0.74	2.36	4.0	1.2	171,000	3.9
95	0.66	2.47	4.5	2.6	113,700	4.4

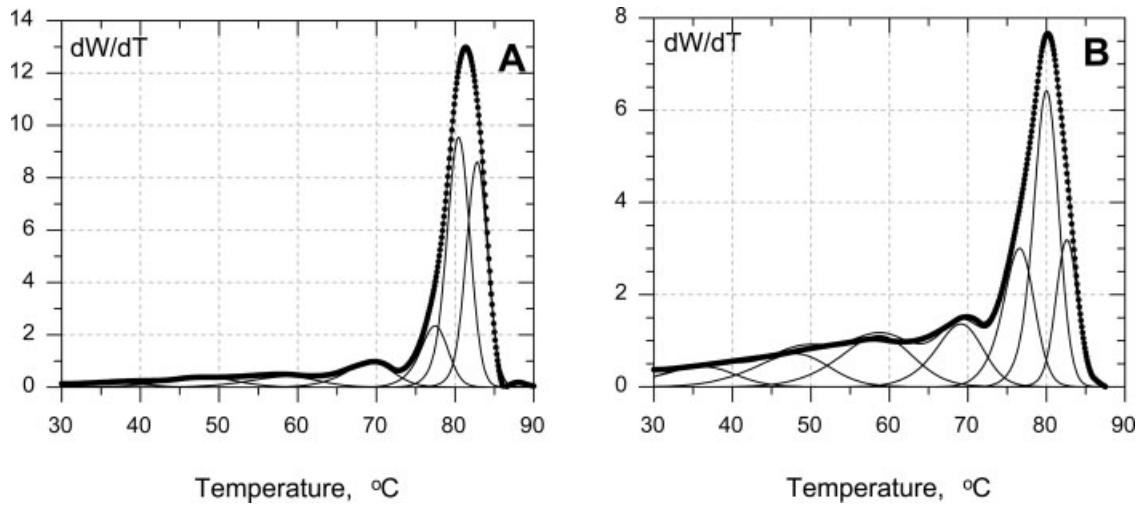

Figure 6 Crystaf curves of ethylene/1-hexene copolymers prepared with a supported Ti-based Ziegler-Natta catalyst at different reaction temperatures and their resolution into elemental components. (A) 75°C, (B) 95°C.

However, much more detailed information can be derived from a parallel analysis of Crystaf and GPC data for these copolymers. Figure 6 shows the Crystaf curves of the two copolymers from Table VI, and Table VII gives the results of the compositional analysis of the respective Crystaf fractions. Figure 7 and Table VIII give the results for the molecular weight distribution analysis of the same two copolymers, from the GPC data. The technique for resolving GPC curves of polymers prepared with multicenter Ziegler-Natta catalysts into elemental Flory components was described earlier in Refs. 10 and 18–22. The comparison of the GPC and Crystaf resolution data confirms that copolymerization reactions of ethylene and α-olefins produce copolymer fractions with vastly different compositions and molecular weights. These fractions can be identified both in Crystaf and in GPC. For example, Crystaf components A and B (the components with very low 1-hexene contents, see Table VII) are the same materials as Flory components IV and V in the GPC data, those with the highest molecular weights. Taking into account difficulties of resolving complex closely spaced Crystaf and GPC curves (see Figs. 6 and 7), the agreement between the two sets of the data is reasonably good: the combined contribution of the Crystaf components A and B in the copolymer prepared at 75°C is ~ 66%, and the combined contribution of the GPC Flory components IV and V is ~ 63%; the respective fractions at 95°C are ~ 38 and 47%, respectively. The Crystaf analysis is much more detailed in the case of the copolymer fractions with relatively high 1-hexene contents: seven such fractions are separated with the Crystaf method whereas only two or three Flory components (components I–III) can be distinguished. The apparent difference between the two techniques is mostly due to the fact that Crystaf components C to G have significantly different compositions (and thus are resolved by Crystaf) but they have relatively close molecular weights and, therefore, are not separated by GPC. As the data in Tables VII and VIII show, the main temperature effect on the multicenter Ziegler-Natta catalyst is a redistribution of the yields of different copolymer components, whereas the compositions and the molecular weights of the components are affected to a much lesser degree (for example, molecular weights of most Flory components decrease with temperature, as expected).[25] Similar conclusions were reached earlier when Tref and GPC data for ethylene/1-butene copolymers prepared with a similar catalyst were compared.[20]

TABLE VII
Temperature Effect on Compositional Distribution of Ethylene/1-Hexene Copolymers Produced with a Supported Ti-Based Ziegler-Natta Catalyst

Temp. (°C)	Component	T_{max} (°C)	C_{Hex} (mol %)	Fraction (%)
75	A	82.8	~0.3	30.1
	B	80.5	0.6	36.3
	C	77.6	0.9	10.3
	D	69.7	1.9	7.5
	E	59.4	3.1	4.6
	F	~ 49	4.3	4.2
	G	~ 37	5.7	1.8
	Soluble fraction[a]			5.3
95	A	82.6	~0.3	11.1
	B	80.1	0.6	26.4
	C	77.8	0.9	14.2
	D	69.5	1.9	10.6
	E	59.4	3.1	13.0
	F	~49	4.3	8.6
	G	~37	5.7	5.3
	Soluble fraction[a]			10.7

[a] Does not precipitate at 30°C.

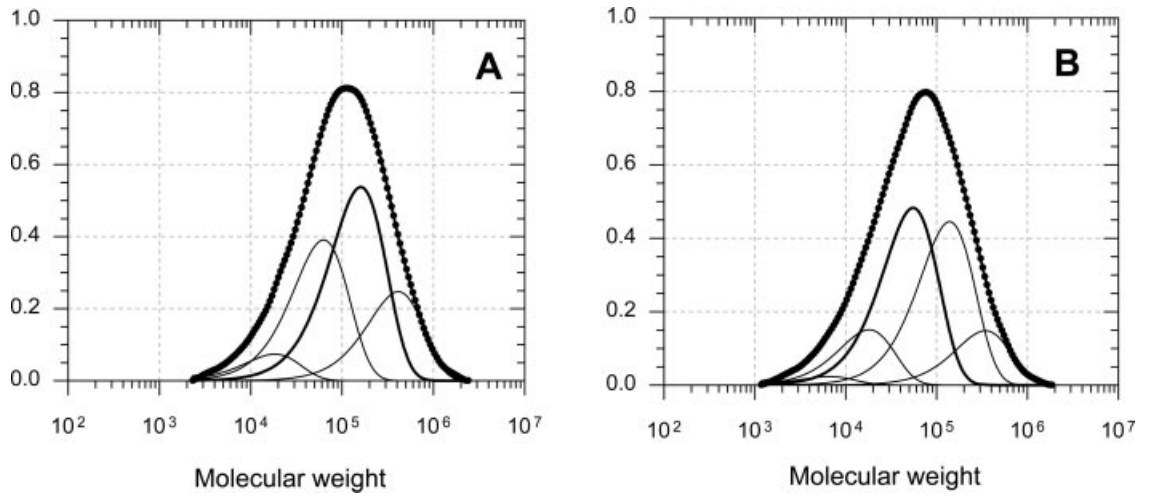

Figure 7 GPC curves of ethylene/1-hexene copolymers prepared with a supported Ti-based Ziegler-Natta catalyst at different temperatures and their resolution into Flory components. (A) 75°C, (B) 95°C.

Ethylene/α-olefin copolymers produced with pseudo-homogeneous catalysts

Figure 8 gives an example of Crystaf analysis of an ethylene/1-hexene copolymer produced with a pseudo-homogeneous catalyst. The transition-metal component in the catalyst is a bidentate complex $LTi(Oi\text{-}Pr)_2$ where L is derived from diphenic acid, and the cocatalyst is a 2 : 1 molar mixture of $AlEt_2Cl$ and MgBu2.[26] The copolymerization reaction was carried out at 70°C, it produced a copolymer with the average 1-hexene content of 3.5 mol %, the average molecular weight of the copolymer, Mw, of $\sim 1.04 \times 105$, and the M_w/M_n ratio ~ 4.9. As Figure 8 shows, nearly 70% of the copolymer is a single Crystaf fraction, a compositionally uniform copolymer material containing 3.2 mol % of 1-hexene.

Isotactic polypropylene

The Crystaf curve-resolution method was also applied to samples of highly isotactic polypropylene prepared with a $TiCl_4/MgCl_2$/1,3-diether catalyst activated with $AlEt_3$. Figure 9 shows one such Crystaf curve. In the case of polypropylene, the dependencies between the T_{max} values of the Gaussian Crystaf peaks and their parameters (peak widths, levels of skew), which were developed for ethylene/α-olefin copolymers, do not apply anymore and the resolution of these curves into elemental components was carried out using a trial-and-error approach. The results give the following information about the sample. The fraction of the highly isotactic material constitutes $\sim$ 91% of the polymer. The product also contains $\sim$ 3% of an amorphous fraction soluble in 1,2,4-trichlorobenzene at 30°C (atactic fraction). As Figure 9 shows, the highly isotactic fraction consists

TABLE VIII
Temperature Effect on Molecular Weight Distribution of Ethylene/1-Hexene Copolymers Produced with a Supported Ti-based Ziegler-Natta Catalyst

Temp. (°C)	GPC component	M_w	Fraction (%)
75	I	–	–
	II	18,300	5.9
	III	62,600	31.3
	IV	160,000	43.0
	V	411,800	19.9
95	I	6,600	1.8
	II	18,000	12.1
	III	55,100	38.6
	IV	138,700	35.6
	V	343,300	11.8

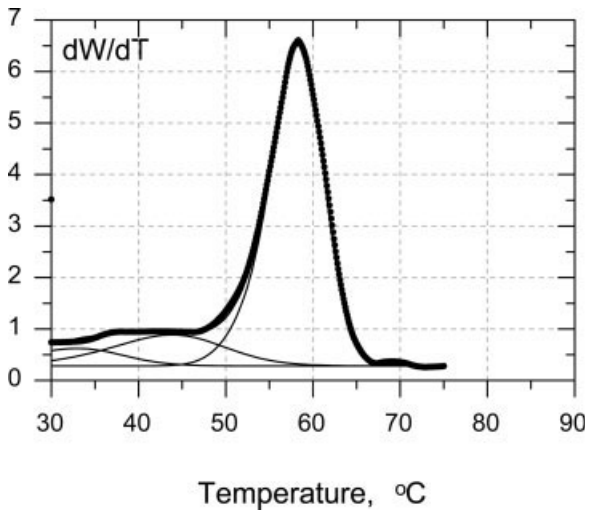

Figure 8 Crystaf curve of an ethylene/1-hexene copolymer (C_{Hex} = 3.5 mol %) prepared with a pseudo-homogeneous Ti-based Ziegler-Natta catalyst (see text) and its resolution into elemental components.

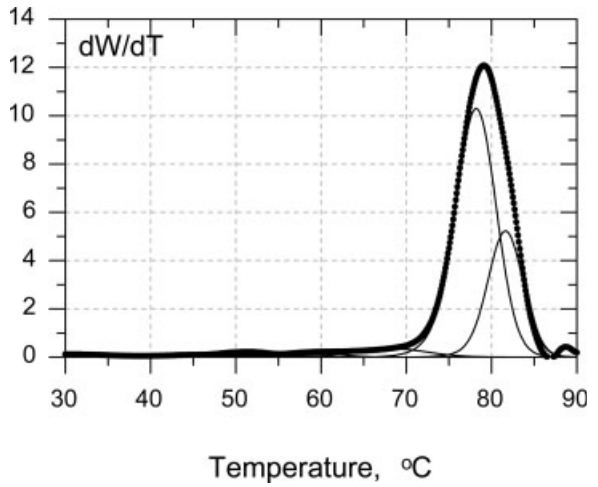

Figure 9 Resolution of the Crystaf curve of polypropylene into components.

of two closely spaced components with T_{max} values 81.8 and 78.3°C in a 1 : 0.44 ratio. A similar nonuniformity of this (nominally, perfectly isotactic) polypropylene fraction was determined earlier by using the analytical Tref method.[27] The polymer also contains three very small fractions of a lower isotacticity. These materials crystallize at 69, ~ 60, and ~ 50°C. After a calibration in the coordinates [*mmmm*] versus T_{max} is developed for polypropylene, such Crystaf data can be used to evaluate catalyst isospecificity in more detail.

Experimental assistance of I. Hook (Edison Research Center, Mobil Chemical Company) is greatly appreciated. Dr. J. H. Paul and Dr. L. B. Joesten (Edison Research Center, Mobil Chemical Company) carried out fractionation of ethylene/1-hexene copolymers by the preparative Tref method. Polypropylene samples were prepared by Dr. M. C. Sacchi (Istituto di Chimica delle Macromolecole, Italy). Dr. A. J. Brandolini (William Paterson University, NJ) recorded NMR spectra of the copolymers.

APPENDIX

Parameters σ of Gaussian curves

The width of Gaussian peaks describing individual Crystaf peaks and the degree of their skewing depend on the position of the peak maximum, T_{max}: the lower is T_{max}, the broader and more skewed is the peak.

Estimation of σ values

The σ values for all peaks in the Crystaf plots were estimated using the following procedure. The Gaussian function [eq. (1)] has the maximum height at T_{max} ($T = 0$) equal to $F(\delta T = 0) = 1/(\sigma\sqrt{2\pi})$. The $\delta T_{1/2}$ value at the half-height of the peak is $0.5F(T_{1/2}) = [(1/(\sigma\sqrt{2\pi})] \cdot \exp[-(\delta T_{1/2})^2/2\sigma^2]$. Dividing the two heights gives $\sigma = \delta T_{1/2}/\sqrt{[-2 \cdot \ln(0.5)]} \cong 0.849\delta T_{1/2}$. High-temperature sides (the sides without the skew) of the Crystaf peaks of several single-center polymers and Tref fractions were used to evaluate approximate σ values. After this, all four parameters for the fractions, T_{max}, δT, σ_{Gauss}, and σ_{skew}, were refined by fitting Crystaf curves of the polymers with weighed sums of eqs. (1) and (2).

Simple empirical dependencies were employed to represent the dependencies between the parameters of skewed Gaussian peaks and T_{max} values.

Variation of σ value

Analysis of the data for compositionally uniform Tref fractions and for single-center polymers, including the data in Ref. 2, shows that the σ_{Gauss} value increases in a nonlinear fashion versus T_{max}. The dependence between σ_{Gauss} and T_{max} values was empirically represented by the equation:

$$\sigma_{Gauss} = A_1 - A_2 \cdot \tan h[A_3 \cdot (T_{max} - T_0)] \qquad (A1)$$

where A_1, A_2, A_3, and T_0 are empirical parameters. The parameters in eq. (A1) depend on the details of the analytical procedure (see Table I as an example) and on the molecular weights of the analyzed polymers; they should be reestimated in every particular case. Under the conditions employed in the above-described experiments, $A_1 = 2.15$, $A_2 = 0.9$, $A_3 = 0.15$, and T_0 (the inflection point on the tanh curve) ~ 61°C.

Parameters of the skew component

The skew of the Crystaf peaks was represented by the second Gaussian peak [eq. (2)]. We assumed that the distance between the main and the skew Gaussian peaks, δT, increases as T_{max} decreases. In the case of ethylene/α-olefin copolymers, the δT value varies linearly from $\delta T_{min} = 1$°C at $T^h_{max} = \sim 83$°C (the crystallization temperature of ethylene homopolymer) to $\delta T_{max} = 4$°C at $T^l_{max} = 30$°C: $\delta T = \delta T_{min} + (\delta T_{max} - \delta T_{min}) \cdot (T^h_{max} - T_{max})/(T^h_{max} - T^l_{max})$. The width of the skew peak was assumed constant, $\sigma_{skew} = 1.3 \cdot \sigma_{Gauss}$. The contribution of the skew component was also assumed to vary linearly: the peaks at high T_{max}, close to T^h_{max}, have no skew and the $R_{skew} = (A_{skew}/A_{Gauss})$ value changes as: $R_{skew} = (R_{skew})_{max} \cdot (T^h_{max} - T_{max})/(T^h_{max} - T^l_{max})$ with $(R_{skew})_{max} = \sim 0.6$.

These parameters were adjusted to produce reasonably satisfactory fits of the Crystaf peak profiles of compositionally uniform ethylene/α-olefin copolymers.

Additional peak broadening for closely spaced peaks

As Figure 3(A) and the data in Table III show, when polymer mixtures containing two compositionally uniform components are analyzed with the Crystaf method, the maximums of both peaks slightly shift toward each other, both peaks become noticeably broader and, as a result, their overlap is much more pronounced. The proposed Crystaf modeling procedure takes some of these changes into account. The corrections were determined by analyzing binary mixtures of Tref fractions in different proportions. Because the Crystaf curves of most polyolefins produced with Ziegler-Natta catalysts consists of a relatively large number of peaks (five to eight, see Figs. 5, 6, and 8) the shifts in positions for most peaks compensate each other. Corrections for two parameters were introduced: (a) the widths of each Gaussian peak in a binary combination (this correction automatically results in broadening of the peaks' skew components), and (b) the fraction of the skew component for the peak with a higher T_{max}. These corrections were formally represented by the following dependencies:

1. The σ_{Gauss} values for both peaks increase, mostly because the fractions co-precipitate. We assumed that the broadening factors for both peaks could be represented by an empirical function which goes through a sharp maximum: the mutual broadening is formally absent when the two peaks have the same T_{max} value, the broadening parameters reach a maximum when the peaks are relatively close, at $T_{max}(1) - T_{max}(2)$ of $\sim$ 6–7°C, and then the broadening effect decreases in a reciprocal relationship to the ΔT value between the two peaks. We assume the same relationship for the R_{skew} ratio for the peak with a higher T_{max} value. All the corrections have the form: corrected value = original value $\cdot F_i$. In the case of σ_{Gauss} values:

$$F(\sigma_{Gauss} = 1 + A\sigma \times K\sigma_1(\exp\{-K\sigma_1 \cdot [T_{max}(1) - T_{max}(2)]^{P\sigma}\} - \exp\{-K\sigma_2 \cdot [T_{max}(1) - T_{max}(2)]^{P\sigma}\}) / (K\sigma_2 - K\sigma_1) \quad (A2)$$

The parameters in eq. (A2) depend on the details of the analytical procedure (see Table I as an example); they should be reestimated for every particular experimental conditions. Under the conditions employed in the above-described experiments:

- for the peak with the higher T_{max} value: $A\sigma = \sim 1.0$, $K\sigma_1 = 0.0301$, $K\sigma_2 = 0.0300$, $P\sigma = 1.85$.
- for the peak with the lower T_{max} value: $A\sigma = \sim 2.0$, $K\sigma_1 = 0.0301$, $K\sigma_2 = 0.0300$, $P\sigma = 1.70$.

2. Another correction factor was introduced for the R_{skew} ratio. It accounts for the distance between the two closely spaced peaks: $(R_{skew})_{corr} = R_{skew} \cdot F_1(A_{skew})$.

$$F_1(A_{skew} = 1 + A_s \times K_1(\exp\{-K_{1s} \cdot [T_{max}(1) - T_{max}(2)]^{Ps}\} - \exp\{-K_{2s} \cdot [T_{max}(1) - T_{max}(2)]^{Ps}\})/(K_{2s} - K_{1s})] \quad (A3)$$

where $A_s = 5.0$, $K_{1s} = 0.022001$, $K_{2s} = 0.022$, Ps = 2.0.

3. The third correction factor for the R_{skew} ratio depends on the relative areas under the two neighboring peaks. It was approximated by the following empirical function of the $A[T_{max}(2)]/A[T_{max}(1)]$ ratio [the peak area ratio of the interfering peak at $T_{max}(1)$ and a given peak at $T_{max}(2)$]. Thus, the final $(R_{skew})_{corr}$ value is $(R_{skew})_{corr} = R_{skew} \cdot F_1(A_{skew}) \cdot F_2(A_{skew})$.

$$F_2(A_{skew}) = 1 + A_{s2} \cdot K_{1s2}(\exp[-K_{1s2} \times \{A[T_{max}(2)]/A[T_{max}(1)]\}^{ps2}]) - \exp[-K_{2s2} \cdot \{A[T_{max}(2)]/A[T_{max}(1)]\}^{ps2}] / (K_{2s2} - K_{1s2}) \quad (A4)$$

where $A_{s2} = \sim 7.5$, $K_{1s2} = 0.767$, $K_{2s2} = 1.556$, P = 1.20.

References

1. Monrabal, B. J Appl Polym Sci 1994, 52, 491.
2. Soares, J. B. P.; Monrabal, B.; Nieto, J.; Blanco, J. Macromol Chem Phys 1998, 199, 1917.
3. Monrabal, B.; Blanco, J.; Nieto, J.; Soares, J. B. P. J Polym Sci Part A: Polym Chem 1999, 37, 89.
4. Britto, L. J. T.; Soares, J. B. P.; Penlidis, A.; Monrabal, B. J Polym Sci Part B: Polym Phys 1999, 37, 539.
5. Stockmayer, W. H. J Chem Phys 1945, 13, 199.
6. Krentsel, B. A.; Kissin, Y. V.; Kleiner, V. I.; Stotskaya, L. L. Polymers and Copolymers of Higher α-Olefins; Hanser: Munich, 1997; Table 8.2.
7. Kissin, Y. V.; Brandolini, A. J. Macromolecules 2003, 36, 18.
8. Kissin, Y. V. J Polym Sci Part A: Polym Chem 2001, 39, 1681.
9. Mink, R. I.; Nowlin, T. E. U. S. Pat. 5,470,812 (1995).
10. Kissin, Y. V.; Mink, R. I.; Nowlin, T. E. J Polym Sci Part A: Polym Chem 1999, 37, 4255.
11. Kissin, Y. V. J Mol Catal 1989, 56, 220.
12. Albizzati, E.; Cecchin, G.; Chadwick, J. C.; Collina, G.; Giannini, U.; Morini, G.; Noristi, L. In Polypropylene Handbook, 2nd ed.; Pasquini, N., Ed.; Hanser: Munich, 2005; Chapter 2.
13. Kamath, P. M.; Wild, L. Polym Eng Sci 1966, 6, 213.
14. Wild, L. Adv Polym Sci 1991, 98, 1.
15. Soares, J. B. P.; Hamilec, A. E. J Appl Polym Sci 1995, 36, 1639.

16. Nowlin, T. E.; Kissin, Y. V.; Wagner, K. P. J Polym Sci Part A: Polym Chem 1988, 26, 755.
17. Provder, T.; Rosen, E. M. Sep Sci 1970, 5, 437 and 485.
18. Anantawaraskul, S.; Soares, J. B. P.; Wood-Adams, P. M. Macromol Chem Phys 2004, 205, 771.
19. Krentsel, B. A.; Kissin, Y. V.; Kleiner, V. I.; Stotskaya, L. L. In Polymers and Copolymers of Higher α-Olefins; Hanser: Munich, 1997; Chapter 8, p 263.
20. Kissin, Y. V.; Mirabella, F. M.; Meverden, C. C. J Polym Sci Part A: Polym Chem 2005, 45, 4351.
21. Kissin, Y. V. Makromol Chem Macromol Symp 1995, 89, 113.
22. Kissin, Y. V.; Mink, R. I.; Nowlin, T. E.; Brandolini, A. J. Topics Catal 1999, 7, 69.
23. Kissin, Y. V.; Mink, R. I.; Nowlin, T. E.; Brandolini, A. J. In Metalorganic Catalysts for Synthesis and Polymerization; Kaminsky, W., Ed.; Springer: Berlin, 1999; p 60.
24. Quijada, R.; Wanderley, A. M. In Catalytic Polymerizations of Olefins; Keii, T.; Soga, K., Eds.; Kadansha: Tokyo, 1986; p 419.
25. Kissin, Y. V. J Polym Sci Part A: Polym Chem 2001, 39, 1681.
26. Mink, R. I.; Kissin, Y. V. U. S. Pat. 5,869,585 (1999).
27. Kissin, Y. V.; Ohnishi, R.; Konakazawa, T. Macromol Chem Phys 2004, 205, 284.